Experimental evidence for a torus breakdown in a glow discharge plasma

C. Letellier
CORIA UMR 6614, Université de Rouen, Place Emile Blondel, F-76821 Mont Saint-Aignan Cedex, France

A. Dinklage,* H. El-Naggar, and C. Wilke
Institut für Physik, Ernst-Moritz-Arndt-Universität Greifswald, Domstrasse 10a, D-17487 Greifswald, Germany

G. Bonhomme
LPMI-CNRS ESA 7040, Université Henri Poincaré, Boîte Postale 239, F-54506 Vandœuvre-lès-Nancy Cedex, France
(Received 29 November 2000; published 29 March 2001)

A global bifurcation scenario for a two-frequency torus breakdown depicted by Baptista and Caldas [Physica D **132**, 325 (1999)] is observed on a glow-discharge experiment. The torus is broken through a crisis with an unstable periodic orbit. The torus section before the bifurcation is a sided polygon that has a number of edges equal to the period of the unstable orbit. Since the discharge is an extended system the two-frequency torus breakdown is shown to be a possible way to space-time chaos.

DOI: 10.1103/PhysRevE.63.042702 PACS number(s): 52.80.Hc, 05.45.−a

Understanding the route to chaos found in nonlinear dynamical systems by varying bifurcation parameters allows one to predict the transition from regular to irregular oscillations. One of the most prominent kinds of bifurcations is associated with torus breakdown as exemplified by the Ruelle and Takens scenario [1]. Among the different possibilities of torus breakdown, there is also the destabilization of a two-frequency torus as proposed by Curry and Yorke [2]. The broken torus presents typical folds and wrinkles. An overview of the possible topological transitions for the two-frequency torus breakdown to chaos may be found in [3,4].

Very recently, a global bifurcation for a two-frequency torus has been reported [5]. The bifurcation appears when the torus grows in size and is broken through a crisis with an unstable periodic orbit. Just before the bifurcation, the torus is constrained by the heteroclinic connections between the periodic points of the unstable orbit. The section of the torus may be viewed as a sided polygon that has a number of edges equal to the period of the unstable orbit. At the bifurcation, there are also heteroclinic connections between the fixed point located near the center of the torus and the unstable periodic points. The trajectory thus spirals out from the inner fixed point and reaches the neighborhood of the unstable periodic orbit. The trajectory is hereafter reinjected near the fixed point through a complicated pattern. This bifurcation has been observed on a Matsumoto-Chua circuit driven by a sinusoidal force [5]. The dynamics is described in a five-dimensional (5D) phase space and this global bifurcation is a tangent bifurcation associated with a type-II intermittency [6]. In this paper, we report on the experimental evidence of that bifurcation in an extended spatiotemporal system.

Experiments were performed in a sealed cylindrical discharge tube (Pyrex glass) that was filled with pure-neon gas at a pressure of $p=3.28$ Torr (273 K). The tube has an internal radius of $r=2.0$ cm and the electrodes (cold hollow cathode and plane anode) were spaced at a distance of $L=70$ cm. Discharge operation was sustained by an external voltage (Fig. 1) and the discharge current I limited by a load resistor ($R=50\,\mathrm{k}\Omega$). If the discharge current I exceeds a low-current threshold, the positive column of the discharge destabilizes through the ionization instability. Current feedback through the external circuit leads to ionization wave resulting in light-intensity fluctuations that can be easily detected by photodiodes or charge-coupled devices. Ionization waves are one-dimensional waves with group velocity directed from cathode to anode, whereas the phase velocity is directed oppositely.

The discharge current I acts as a bifurcation parameter and variations of I allows one to observe coherent waves, quasiperiodic regimes, weak space-time chaos and developed defect turbulence [7]. Oscillations of the near-cathode region of the positive column (column head) inject high-frequency ionization wave that decays towards the anode into a low-frequency eigenmode. Irregularity depends on commensuration of the injected high frequency wave (cathode side) and the low-frequency eigenmode (anode side). Since the plasma

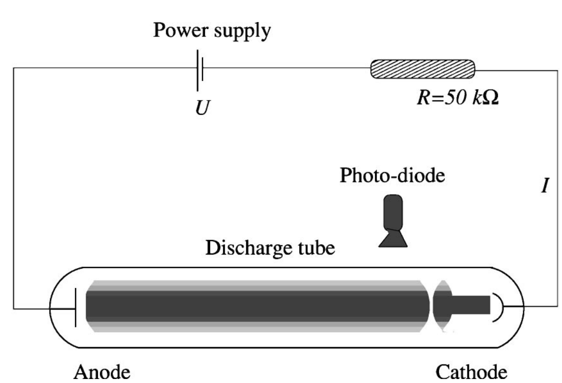

FIG. 1. Experimental setup. The light fluctuations are recorded near the cathode with a sampling rate of 500 kHz.

*Present address: Max-Planck-Institut für Plasmaphysik, EURATOM Association, Teilinstitut Greifswald, Wendelsteinstrasse I, 17491 Greifswald, Germany

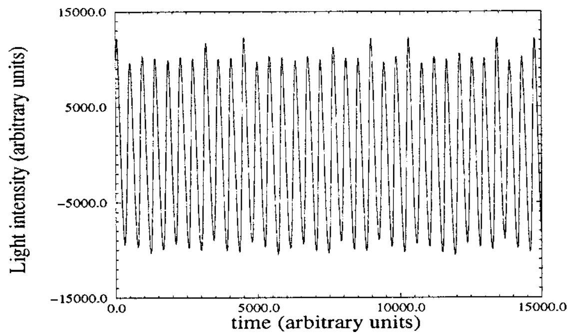

FIG. 2. Time series of the light intensity recorded near the cathode by using a photodiode ($I = 30.4$ mA).

parameters do not vary significantly over a large current range ($15 < I < 50$ mA) the eigenfrequency does not vary as well. But the column-head oscillation frequency increases linearly with increasing discharge current. Consequently, varying the bifurcation parameter I modifies the ratio of column-head frequency and fixed eigenfrequency. It should be noted that the oscillation of the column head is owing to internal discharge mechanism, hence the plasma is said to be internally driven. In the following we focus on the dynamics in the near-cathode region, i.e., the column head.

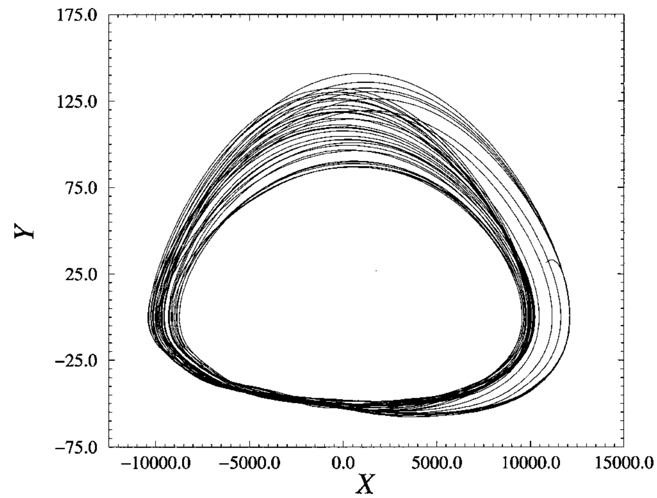

FIG. 3. Plane projection of the reconstructed phase space spanned by derivative coordinates ($I = 30.4$ mA).

When the discharge current I is varied from 28.2 to 33.0 mA, the following regimes can be observed. A period-3 phase-locked attractor ($I = 28.2$ mA), a period-6 phase-locked attractor ($I = 28.4$ mA), a quasiperiodic regime ($28.6 < I < 29.8$ mA), a period-10 phase-locked attractor (I

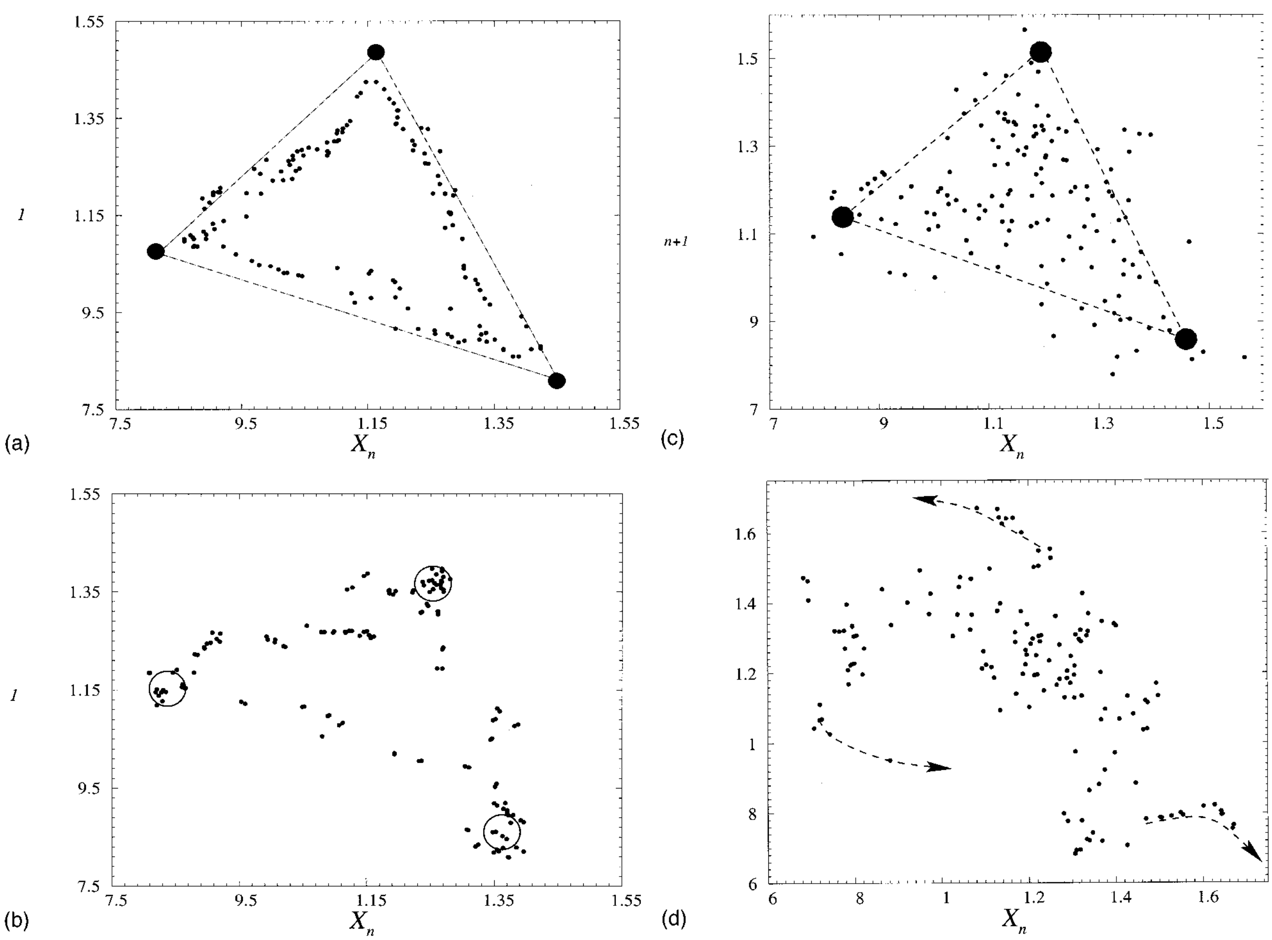

FIG. 4. First-return maps to the Poincaré section for four different values of the discharge current I. The three unstable periodic points are drawn by hand in order to clarify the relative organization between the torus and the unstable periodic orbit. The heteroclinic connections are represented by dashed lines. 130 points are recorded in the Poincaré section.

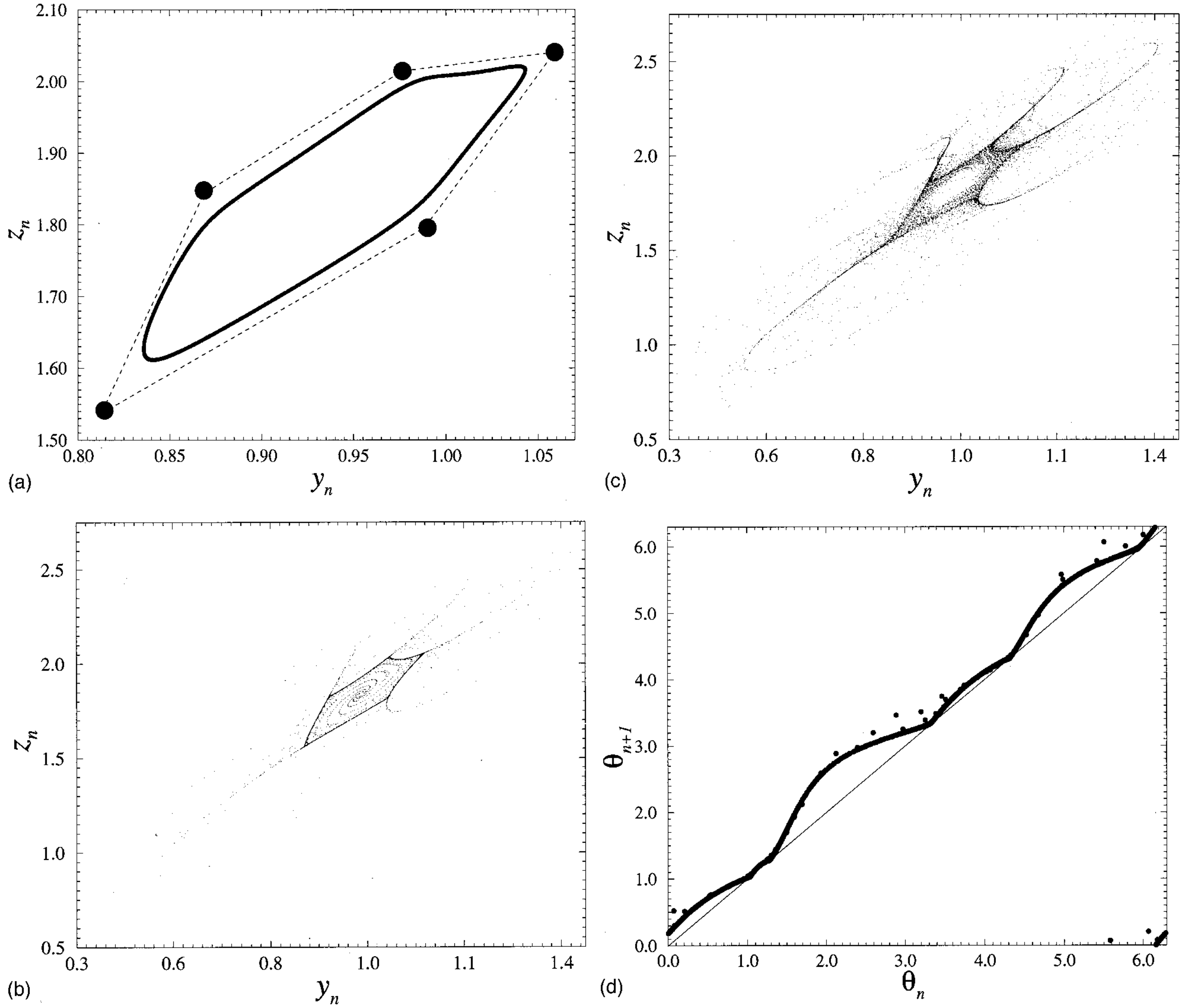

FIG. 5. Evolution of the torus breakdown through the global bifurcation as observed in the Matsumoto-Chua circuit by Baptista and Caldas. 200 000 points are used for these figures.

$=30.0\,\mathrm{mA}$), a torus breakdown ($I=30.2\,\mathrm{mA}$), and a chaotic attractor ($30.4<I<33.6\,\mathrm{mA}$). In this paper, we will mainly focus our attention on the global bifurcation inducing the two-frequency torus breakdown at a discharge current of about $I=30.2\,\mathrm{mA}$.

A typical time series of the light fluctuations $L(t)$ is displayed in Fig. 2 for $I=30.4\,\mathrm{mA}$. The first step of any qualitative analysis is to reconstruct a phase space from the recorded time series at a sampling frequency of 500 kHz (Fig. 3). We choose to employ the derivative coordinates ($X=L$, $Y=\dot{L}$, $Z=\ddot{L}$). The quality of the experimental time series allows one to determine the successive time derivatives analytically by fitting a polynomial through the experimental data. For this purpose we used a singular value decomposition technique for windows centered at all-time instants where the derivatives have to be calculated. The time series is slightly smoothed before. The number of dynamical variables required for an unambiguous description of the dynamics is estimated by computing the embedding dimension using a false nearest neighbors technique [8]. We found a minimum-embedding dimension of 5 or 6. Nevertheless, the 3D subspace spanned by $X=L$, $Y=\dot{L}$, and $Z=\ddot{L}$ will be sufficient to exhibit the main characteristics of the global bifurcation.

In the subspace $\mathbb{R}^3(X,Y,Z)$, the dynamical structure is investigated by means of the first-return map to the Poincaré section

$$P\equiv\{(Y_n,Z_n)\in\mathbb{R}^2|X_n=0,\dot{X}_n>0\}. \tag{1}$$

When the discharge current is increased from $I=28.6$ to 29.8 mA, the torus grows in size and approaches the heteroclinic connections between the periodic points of a period-3 unstable orbit. Its shape is thus constrained to look like a three-sided polygon as shown in Fig. 4(a) where the periodic points and the heteroclinic connections are drawn for the sake of clarity. When the discharge current is set to 30.2 mA, the trajectory spends most of its time close to the three unstable periodic points [Fig. 4(b)]. This feature is typical for a tangent bifurcation associated with an intermittency, involving an unstable period-3 orbit. Unfortunately, the stepsize used for varying the bifurcation parameter ($\delta I = 0.2\,\mathrm{mA}$) is not sufficiently small for locating more precisely the bifurcation.

For comparison we discuss a similar scenario in a purely temporal system. Indeed, let us mention that Baptista and Caldas used the fifth decimal of the amplitude voltage of the driving force to identify the global bifurcation they observed in their numerical simulations of a Matsumoto-Chua circuit [6]. The Matsumoto-Chua circuit and the bifurcation parameters values are described in [5,6]. This global bifurcation for the two-frequency torus breakdown has been analyzed using the same diagnostic tools as for the experimental data (Fig. 5).
Only the amplitude of the driving external force is here reported for illustrating the accuracy required for identifying all characteristics of such a global bifurcation. First, a quasiperiodic motion is observed. The corresponding torus has a section that is constrained by the heteroclinic connections between the periodic points of an unstable period-5 orbit [Fig. 5(a)].

At the bifurcation, there is a heteroclinic orbit that spirals out from a periodic point near the center of the torus and toward the unstable periodic orbits [Fig. 5(b)]. The trajectory is finally reinjected in the neighborhood of the inner periodic points following the heteroclinic connections between the unstable manifolds associated with the periodic points and the stable manifold of the inner point. The unstable manifolds spiral around the region occupied by the broken torus [Fig. 5(c)]. We have computed the angular fifth-return map slightly before the tangent bifurcation. Five tangencies with the bisecting line are identified as expected [Fig. 5(d)].

For the discharge experimental evidence of the tangent bifurcation is exhibited by using an angular third-return map to the Poincaré section (Fig. 6). Near the bifurcation, the angular third-return map is nearly tangent to the bisecting line in three points (Fig. 6). Shortly after the bifurcation, the torus is filled [Fig. 4(c)] and when the bifurcation parameter is increased up to $I = 31.0\,\mathrm{mA}$ the trajectory visits the unstable manifold associated with the periodic points of the period-3 orbit [Fig. 4(d)] in a similar way as observed in the numerical Matsumoto-Chu circuit [Fig. 5(c)], i.e., three branches [indicated by the arrows in Fig. 4(d)] are observed spiralling around the region where the torus was.

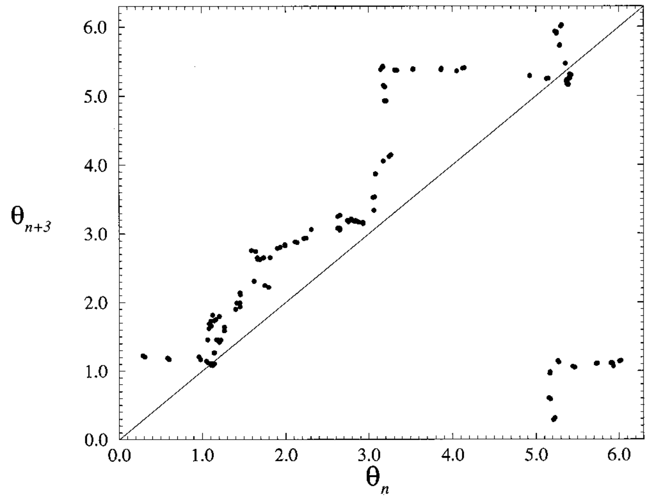

FIG. 6. Anuglar third-return maps to the Poincaré section. Three tangencies with bissecting line are identified. They confirm the dominant role played by an unstable period-3 orbit.

Concluding, we give experimental evidence for a global bifurcation inducing a two-frequency torus breakdown (as previously depicted by Baptista and Caldas in numerical simulations [6]) in a glow discharge representing an extended, spatiotemporal system. Three characteristic features have been identified clearly, (i) a torus section resembling to a sided polygon, (ii) a tangent bifurcation exhibited by an angular third-return map, and (iii) three unstable manifolds spiralling around the region where the torus was before the bifurcation. The stepsize of the bifurcation parameter, i.e., of the discharge current I cannot be chosen sufficiently small due to experimental limitations in order to identify where the bifurcation exactly occurs and, consequently, the type-II intermittency that should be associated with this bifurcation cannot be identified. Nevertheless, our findings clearly confirm that the two-frequency torus breakdown is a possible way not only to temporal chaos but also to space-time chaos.

C.L. thanks E. Macau for pointing out the papers by M. Baptista and I. Caldas and the latter for enlightening discussions during his stay at the Universidade Federale de Minas Gerais (Brazil) supported by CNRS and CNPq. The German team is supported by the Deutsche Forschungsgemeinschaft through SFB 198.

[1] D. Ruelle and F. Takens, Commun. Math. Phys. **20**, 167 (1971).
[2] J. H. Curry and J. A. Yorke, Lect. Notes Math. **668**, 48 (1978).
[3] D. G. Aroson, M. A. Chory, G. R. Hall, and R. P. McGhee, Commun. Math. Phys. **83**, 303 (1982).
[4] S. Ostlund, D. Rand, J. Sethna, and E. Siggia, Physica D **8**, 303 (1983).
[5] M. S. Baptista and I. L. Caldas, Phys. Rev. E **58**, 4413 (1998).
[6] M. S. Baptista and I. L. Caldas, Physica D **132**, 325 (1999).
[7] A. Dinklage, C. Wilke, G. Bonhomme, and A. Atipo, Phys. Rev. E **62**, 7219 (2000).
[8] L. Cao, Physica D **110**, 43 (1997).